ESMO GOOD SCIENCE BETTER MEDICINE BEST PRACTICE

ESMO OPEN CANCER HORIZONS

ORIGINAL RESEARCH

# Assessing the impact of organ-specific lesion dynamics on survival in patients with recurrent urothelial carcinoma treated with atezolizumab or chemotherapy

M. Kerioui[1,2,3,4*], S. Desmée[2], F. Mercier[5], A. Lin[6], B. Wu[6], J. Y. Jin[6], X. Shen[7], C. Le Tourneau[8], R. Bruno[9] & J. Guedj[1]

[1]Université de Paris, INSERM IAME, Paris; [2]Université de Tours, Université de Nantes, INSERM SPHERE, UMR 1246, Tours; [3]Institut Roche, Boulogne-Billancourt; [4]Clinical Pharmacology, Genentech/Roche, Paris, France; [5]F. Hoffmann-La Roche AG, Biostatistics, Basel, Switzerland; [6]Clinical Pharmacology, Genentech Inc., South San Francisco; [7]Product Development, Genentech Inc., South San Francisco, USA; [8]Department of Drug Development and Innovation (D3i), INSERM U900 Research Unit, Paris-Saclay University, Paris & Saint-Cloud; [9]Clinical Pharmacology, Genentech/Roche, Marseille, France

Available online xxx

**Background:** Tumor dynamics typically rely on the sum of the longest diameters (SLD) of target lesions, and ignore heterogeneity in individual lesion dynamics located in different organs.

**Patients and methods:** Here we evaluated the benefit of analyzing lesion dynamics in different organs to predict survival in 900 patients with metastatic urothelial carcinoma treated with atezolizumab or chemotherapy (IMvigor211 trial).

**Results:** Lesion dynamics varied largely across organs, with lymph nodes and lung lesions showing on average a better response to both treatments than those located in the liver and locoregionally. A benefit of atezolizumab was observed on lung and liver lesion dynamics that was attributed to a longer duration of treatment effect as compared to chemotherapy ($P$ value = 0.043 and 0.001, respectively). The impact of lesion dynamics on survival, assessed by a joint model, varied greatly across organs, irrespective of treatment. Liver and locoregional lesion dynamics had a large impact on survival, with an increase of 10 mm of the lesion size increasing the instantaneous risk of death by 12% and 10%, respectively. In comparison, lymph nodes and lung lesions had a lower impact, with a 10-mm increase in the lesion size increasing the instantaneous risk of death by 7% and 5%, respectively. Using our model, we could anticipate the benefit of atezolizumab over chemotherapy as early as 6 months before the end of the study, which is 3 months earlier than a similar model only relying on SLD.

**Conclusion:** We showed the interest of organ-level tumor follow-up to better understand and anticipate the treatment effect on survival.

**Key words:** cancer clinical trials, nonlinear mixed-effects model, survival prediction, joint model, immunotherapy

## INTRODUCTION

Urothelial carcinoma is the ninth most common cancer in the world with a 5-year survival of 77% all stages combined, but this rate drops to 5% for metastatic diseases.[1] Immunotherapy treatments have shown impressive results in the past few years in several cancers including urothelial carcinoma.[2-6] However, a number of analyses have also emphasized the large variability in the response observed, which may complicate the assessment of immunotherapy efficacy.[7] This may in particular be due to the intra-patient variability, with some lesions responding and some progressing within one patient.[8,9] More generally, the lesion location could also affect the overall tumor burden[10] and the risk of death.[11]

This questions the limitations of the sum of the longest diameters (SLD) to evaluate the response to treatment. Indeed, this marker, which is key to calculate RECIST criterion (Response Evaluation Criteria In Solid Tumors),[12] lumps together the dynamics of the target lesions and potentially masks the heterogeneity in individual lesions.[13]

In order to analyze complex relationship between target lesion dynamics, organ location and survival,[14] one approach is joint models, which simultaneously handles longitudinal and time-to-event data.[15,16] This approach can provide a precise estimation of the association between nonlinear SLD dynamics and survival[17] and help in early identification of most at-risk patients.[18,19] Another approach is the Cox regression model, but it is not appropriate for a time-dependent covariate, as it assumes a piecewise linear trajectory of the biomarker, neglects the

*Correspondence to: Marion Kerioui, UMR 1137, UFR de Médecine Paris 7 Denis Diderot, 16 rue Henri Huchard, B.P. 416, 75870 Paris cedex 18, France
E-mail: marion.kerioui@inserm.fr (M. Kerioui).

measurement error and might lead to a biased estimation of the association parameter.[16]

Here, we aimed to extend this approach to analyze target lesion dynamics in each organ and their specific effect on survival. Applied to data from a phase III clinical trial (IMvigor211[20]) comparing the efficacy of atezolizumab and chemotherapy on overall survival (OS) in patients with platinum-treated advanced or metastatic urothelial carcinoma, we evaluated whether individual organ tumor dynamics could improve survival prediction and enable a better anticipation of the treatment efficacy.

## METHODS

### Data

The phase III clinical trial IMvigor211[20] included 931 patients with advanced or metastatic urothelial carcinoma, randomized to two treatment arms; 464 patients were assigned to the control chemotherapy arm and 467 patients were assigned to the atezolizumab immunotherapy arm. Among patients in the chemotherapy arm, 242 (52%) received vinflunine, 148 (32%) received paclitaxel and 53 (11%) patients received docetaxel. Patients who did not receive treatment were excluded from our analysis (21 patients in the control arm and 8 in the atezolizumab arm), as well as those who did not have any target lesion measurement (2 patients in the atezolizumab arm). Thus, a total of $N = 900$ patients were included in our analysis—443 in the chemotherapy arm and 457 in the atezolizumab arm (Supplementary Figure S1, available at https://doi.org/10.1016/j.esmoop.2021.100346).

According to RECIST, there was a maximum of five target lesions followed in each individual with a maximum of two per organ. Assessment of target lesions was done at study inclusion, every 9 weeks during the first year and every 12 weeks afterward, with a limit of quantification of 2.5 mm. Disease progression, following RECIST, led to clinical follow-up discontinuation but the survival status continued to be collected. However, trial protocol permitted patients demonstrating clinical benefit from atezolizumab to continue treatment beyond disease progression.

Before the analysis and given the quantity of data available in the different organs, four locations were considered: lymph nodes, lung or pleura (called 'lung' in the following), liver and bladder or pelvis or peritoneum (called 'locoregional' in the following). All other lesions were lumped together (called 'other' in the following). For each organ, the sum of the longest diameters (SLD) was computed, and we referred to these quantities as organ-specific SLD.

Baseline covariates are summarized in Table 1.

**Table 1. Baseline characteristics of patients**

| | Chemotherapy | Atezolizumab |
|---|---|---|
| Data description | | |
| Analysis population (patients) | 443 | 457 |
| Death (proportion %) | 343 (77) | 317 (69) |
| Number of target lesions | 1064 | 1069 |
| Total SLD measurements | 1317 | 1662 |
| Number of SLD assessments per patient (median, min-max) | 2 (1-12) | 3 (1-11) |
| Categorical covariates | Proportion, % (count) | |
| Female sex | 22 (97) | 23 (107) |
| Baseline ECOG Score = 1 | 56 (246) | 53 (242) |
| ≤5% of PD-L1 positive immune cells | 25 (112) | 25 (113) |
| Previous therapy with platinum-based regimen | | |
| Cisplatin-based | 56 (247) | 56 (255) |
| Carboplatin-based | 44 (195) | 42 (192) |
| Other platinum combination | <1 (1) | 2 (9) |
| Continuous covariates | Median (min-max) | |
| Age (years) | 67 (31-84) | 67 (33-88) |
| Baseline albumin concentration (g/l) | 39.1 (3.1-66.7) | 40.0 (20.1-49.0) |
| Baseline alkaline phosphatase (U/l) | 96 (40-623) | 92 (36-571) |
| Baseline lactate dehydrogenase value (U/l) | 214.0 (98.0-3000.0) | 208.0 (0.8-1500.0) |
| Baseline neutrophil-to-lymphocyte ratio | 3.70 (0.56-58.53) | 3.48 (1.06-59.72) |
| Baseline C-reactive protein (mg/l) | 14.40 (0.31-314.0) | 14.50 (0.40-178.0) |
| Baseline hemoglobin concentration (g/l) | 119.0 (84.0-163.0) | 121.0 (82.2-162.0) |
| Organ-specific data | | |
| Patients having at least one target lesion in the | | |
| Lymph nodes | 218 | 209 |
| Lung | 154 | 156 |
| Liver | 125 | 130 |
| Locoregional area | 94 | 87 |
| Other | 111 | 115 |
| Death in patient having at least one target lesion in the (%) | | |
| Lymph nodes | 76 | 62 |
| Lung | 77 | 72 |
| Liver | 90 | 83 |
| Locoregional area | 86 | 70 |
| Other | 84 | 79 |
| Total number of SLD measurements in the | | |
| Lymph nodes | 709 | 835 |
| Lung | 432 | 567 |
| Liver | 307 | 384 |
| Locoregional area | 238 | 321 |
| Other | 312 | 384 |

ECOG, Eastern Cooperative Oncology Group; PD-L1, programmed death ligand-1; SLD, sum of the longest diameters.

### Longitudinal model for organ-specific SLD kinetics

**Structural model.** We used the simplified tumor growth inhibition (sTGI) model[21] to describe organ-specific tumor dynamics in each location $m \in \mathcal{M}$, with $\mathcal{M} = \{$lymph nodes, lung, liver, locoregional, other$\}$. At patient inclusion at time $t = 0$, the model assumes an exponential growth $g_m$ of tumor size in the absence of treatment. At treatment initiation ($t = t_x$), the model assumes a tumor growth inhibition with rate $\varepsilon_m$, and the treatment effect decreases over time (e.g. due to treatment resistance) with rate $c_m$, as followed:

$$SLD_m(t) = \begin{cases} BSLD_m\, e^{g_m t} & t < t_x \\ BSLD_m \exp\left(g_m t - \frac{\varepsilon_m}{c_m}\left(1 - e^{-c_m(t-t_x)}\right)\right) & t \geq t_x \end{cases} \quad (1)$$

where $SLD_m$ is the function of the SLD of the target lesions in organ $m$ at time, and $BSLD_m$ is the baseline SLD (i.e. at $t = 0$) in organ $m$.

**Nonlinear mixed-effects model.** We denoted $y_{ijm}$ the $j^{th}$ measurement of SLD at time $t_{ijm}$ in organ $m$ of individual $i$ and the model was defined as:

$$\begin{aligned} y_{ijm} &= SLD_m(t_{ijm},\ \Psi_{mi}) \\ &\quad + (\ \sigma_{inter_m} + \sigma_{slope_m} SLD_m(t_{ijm},\ \Psi_{mi}))e_{ijm} \end{aligned} \quad (2)$$

where $SLD_m$ is the function of the sTGI structural model defined in equation (1), $e_{ijm}$ a Gaussian residual error term, and the parameters $\sigma_{inter_m}$ and $\sigma_{slope_m}$ are the additive and multiplicative components of the error model for organ $m$. The individual parameters vector $\Psi_{mi}$ of patient $i$ in the organ $m$ depends on a fixed population effect vector $\mu_m = \{\mu_{BSLD_m},\ \mu_{g_m},\ \mu_{\varepsilon_m}, \mu_{c_m}\}$ representing a median effect in organ $m$ and a patient random effect $\eta_{mi} \sim N(0,\ \Omega_m)$. The variance–covariance matrix $\Omega_m$ with the diagonal components $\omega^2_{q_m}$ describes the inter-patient variability for parameter $q \in \{BSLD,\ g, \varepsilon, c\}$ in the organ $m$. The global variance–covariance matrix $\Omega$ is a block-diagonal matrix and its main-diagonal blocks are the diagonal matrix $\Omega_m$. The four parameters being positive by definition, we assumed a log-normal distribution on all parameters:

$$\log(\Psi_{q_m i}) = \log(\mu_{q_m}) + \eta_{q_m i} + \alpha_{q_m} X_{l,i}$$

$$\Psi_{q_m i} = \exp(\ \log(\mu_{q_m}) + \eta_{q_m i} + \alpha_{q_m} X_{l,i}\ ) \quad (3)$$

with $\alpha_{q_m}$ the impact of longitudinal covariate $X_l$ on parameter $q$ in organ $m$. Following previous definitions, the total SLD model that describes the total SLD of the target lesions, regardless of tumor location, was defined as:

$$y_{ij} = SLD(t_{ij},\ \Psi_i) + (\ \sigma_{inter} + \sigma_{slope} SLD(t_{ij},\ \Psi_i))e_{ij} \quad (4)$$

### Impact of organ-specific tumor dynamics on survival

The joint model assumed a current SLD link function (i.e. the SLD at time $t$ impacts the hazard at time $t$) in the individual hazard function $h(t,\Psi_i)$:

$$h(t,\ \Psi_i) = h_0(t) \exp\left(\sum_{m \varepsilon \Lambda} \beta_m SLD_m(t,\ \Psi_{i,m})\right) \quad (5)$$

where $\Psi_i$ is the individual vector of organ-specific individual parameters of patient $i$ and $h_0$ is a baseline parametric hazard function. The link parameters $\beta_m$ capture the strength of the association between the tumor dynamics in organ $m$ and the instantaneous risk of death. A null link parameter $\beta_m = 0$ refers to a 'no link model' that assumes no association between the tumor size in organ $m$ and OS. Of note, if an individual $i$ has no target lesion in organ $m$, then $SLD_m = 0$ with no impact on its survival probability.

### Tumor dynamics model selection

For the sake of calculation, the covariates selection model, including type of treatment received, was built on the total SLD model defined in equation (4). Continuous covariates were centered to their respective mean value and were imputed to the median value in case of missing data. A first screening of baseline covariates was done using a correlation test between the empirical Bayes estimates of the individual parameters and the vector of covariates at level 0.10 (Pearson/Spearman correlation test for continuous/categorical covariates). Then, a forward selection was used in baseline covariates previously selected in the screening, until the improvement in Bayesian information criteria (BIC) was less than two points (corresponding here to a likelihood ratio test at level 0.003). Finally, an effect of atezolizumab was tested on the treatment-related parameters, $\varepsilon$ and $c$, and was retained in case of BIC improvement.

The covariates model identified using the total SLD dynamics was then used as a baseline model for each organ-specific model. Then, we investigated whether parameters were correlated across organs, introducing non-null covariance terms $\omega_{q_m q_{m'}}$ between the $q$ parameters of two different organs $m$ and $m'$. A first screening was done based on a Pearson correlation test at level 0.10 in the model without any correlation. Finally, a forward procedure based on BIC was carried out consistent with the covariates selection strategy described earlier.

### Joint model selection

OS was modelled using a proportional hazard model with a Weibull baseline hazard function, of shape $k$ and scale $\lambda$.[19] Baseline covariates were first included in the baseline hazard function [$h_0$ in equation (5)] in a multiplicative exponential term, as follows:

$$h_{0,i}(t) = \frac{k}{\lambda}\left(\frac{t}{\lambda}\right)^{k-1} \exp\left(\sum_{s=1}^{S} \gamma_s X_{s,i}\right) \quad (6)$$

with $\gamma_s$ the coefficient associated to covariate $X_s$, for all the $S$ survival covariates. In line with the longitudinal submodel, baseline covariates were selected in a forward procedure on BIC. Then, we included the tumor dynamics specific to each organs in the hazard function (5) in a forward procedure until the BIC improvement was less than two points. Finally, atezolizumab effects were tested in a forward procedure on the shape survival parameters $k$, and as a baseline covariate in the $h_0$ function in equation (6) (Wald test). In the final

joint model, baseline covariates, atezolizumab effects and correlations whose *P* value was greater than 0.05, were removed in a backward procedure (Wald Test).

### *Parameters estimation and model evaluation*

Joint models population parameters were estimated with the Stochastic Approximation of Expectation-Maximization (SAEM) algorithm[22] implemented in the Monolix software (2018 R2, Lixoft http://www.lixoft.eu/). Diagnostic plots[23] were carried out using R software (version 3.6.0).

**Derived metrics.** We defined the tumor-size progression-free survival metrics to describe the individual behavior of the disease under treatment. It was computed as the time for the model-predicted organ-specific SLD to reach 120% of its nadir value ($1.2 \times NADIR$), or the observed time of death, whichever comes first. The nadir measurement is defined as the minimal value reached by the organ-specific SLD, and might be equal to the baseline measurement in the absence of tumor decrease under treatment. This metric is largely inspired from the progression-free survival, which is widely used in oncology clinical trials, but differs from it by relying on the organ-specific SLD and not accounting for any other markers of disease progression such as appearance of new lesions. However, it gives an idea of the duration of time during which patients respond to treatment or at least remain stable, at the organ level.

### *Prediction of treatment efficacy on overall survival*

We aimed to assess the benefit of organ-specific tumor dynamics to predict early the effect of atezolizumab.[24] We relied on the hazard ratio (HR) based on observed OS data using a Cox regression model to assess the treatment effect significance (see Supplementary Material, available at https://doi.org/10.1016/j.esmoop.2021.100346).

To investigate this question, we re-estimated joint model parameters assuming that data (SLD measurements and survival events) were available only until a given cut-off time. Since the last patient inclusion was on 15 February 2016, we considered a cut-off time of (i) 15 May 2016 (i.e. 3 months after the last patient inclusion), (ii) 13 August 2016 (i.e. 6 months after last patient inclusion), (iii) 11 November 2016 (i.e. 9 months after last patient inclusion) and (iv) 17 March 2017 (i.e. the entire dataset used in the principal analysis, 13 months after last patient inclusion). At each cut-off time, parameter estimates were used to simulate 1000 clinical datasets up to 13 months after last patient inclusion (i.e. final cut-off in the principal analysis). Individual parameters were drawn in their population distribution, using baseline characteristics from the original dataset. For each simulated clinical trial, SLD measurements and time-to-death were sampled from individual distributions derived from the simulated individual parameters.

The simulated survival data thus generated were analyzed using a Cox regression model and we calculated the HR associated with atezolizumab compared to chemotherapy. We used the same approach as the one used in the primary clinical trial data analysis,[20] with stratification factors being the presence of liver metastases and programmed death ligand-1 (PD-L1) expression (<5% of tumor-infiltrating immune cells). This procedure was repeated on the 1000 simulated datasets to calculate the median HR and the 95% prediction interval (PI), for each cut-off date.

The same procedure was used to generate median HR and 95% PI based on the joint model relying on the total SLD defined in equation (4). Finally, at each cut-off time, the observed HR and its 95% confidence interval (CI) obtained in an interim analysis using only the survival data available in a Cox regression model were compared to the median HR and their 95% PI obtained using longitudinal and survival data available.

## RESULTS

### *Exploratory results*

Less than 4% of the total baseline covariates were missing, and were imputed to their median values. Baseline characteristic distributions were similar in both treatment arms (Table 1).

A total of 2133 target lesions were followed over time, including 1064 in the chemotherapy arm and 1069 in the atezolizumab arm. Overall, 2979 measurements of total SLD were available, with 1317 being measured in the chemotherapy control arm, and 1662 in the atezolizumab arm, with a median (min-max) of 2 (1-12) measurements per patient in the chemotherapy control arm, as compared to 3 (1-11) measurements in the atezolizumab arm. A total of 4489 organ-specific measurements were available, including 1544 measurements in the lymph, 999 in the lung, 691 in the liver, 559 in the locoregional area and 696 in other location.

Overall, 427 patients had at least one lymph node target lesion (47%), 310 patients had at least one lesion near or in the lung (34%), 255 patients had at least one liver lesion (28%) and 181 patients had a locoregional recurrence (20%), with no differences between the two treatment arms. Of note, 43% of the intent-to-treat population underwent a cystectomy before inclusion.[20]

More than half patients had only one target lesion location (57%), 283 (31%) had two target lesion locations and only 102 patients (11%) had three target lesion locations or more. The most frequent combination was lymph node and lung, with 98 patients having target lesions in both organs (Supplementary Figure S2, available at https://doi.org/10.1016/j.esmoop.2021.100346).

At the end of the study, 343 patients (77%) had died in the chemotherapy arm and 317 patients (69%) in the atezolizumab arm (Table 1). Using a Cox regression model, the HR (95% CI) in the analysis population was 0.82 (0.71-0.96) in favor of atezolizumab (Figure 1A), similar to the intent-to-treat population [0.85, (0.73-0.99), Supplementary Figure S1, available at https://doi.org/10.1016/j.esmoop.2021.100346].[20]

The median OS was 257 days in the chemotherapy arm and 280 days in the atezolizumab arm. It was much shorter

in patients having liver target lesions, with 171 days in the chemotherapy arm and 136 days in the atezolizumab arm. In contrast, patients having lymph nodes target lesions had a better survival prognosis, with a median OS up to 357 days in the atezolizumab arm. Regardless of location, a faster drop in the OS was observed in the early treatment times in patients receiving atezolizumab compared to chemotherapy, while OS was higher in the atezolizumab arm at later times (Figure 1).

### *Organ-specific tumor dynamics*

The organ-specific SLD joint model captured well the individual tumor dynamics in all organs (Supplementary Figure S6, available at https://doi.org/10.1016/j.esmoop.2021.100346) despite the high diversity of patients' profiles (Supplementary Figures S3, S7-S10, available at https://doi.org/10.1016/j.esmoop.2021.100346). The model could also capture the diversity of lesion dynamics within each patient, with some responding and some being resistant to treatment (Supplementary Figure S4, available at https://doi.org/10.1016/j.esmoop.2021.100346).

Tumor characteristics varied across organs, with a larger baseline size in the liver and locoregionally (population median $BSLD = 40.4\ mm$ and $46.7\ mm$ respectively), than in the lymph or the lung (population median $BSLD = 31.9\ mm$ and $33.2\ mm$, respectively).

The treatment effect strength and durability also varied across organs. Indeed, the shrinkage of the tumor size was nearly twice as fast in the lymph and the lung (population median up to $\varepsilon = 0.0050\ \text{day}^{-1}$ in the lymph nodes) than in the liver and locoregionally ($\varepsilon = 0.0020\ \text{day}^{-1}$ and $\varepsilon = 0.0017\ \text{day}^{-1}$, respectively). In addition, resistance appearance was at least three times faster in the lung, liver and locoregional tumors than in the lymph nodes (population median $c = 0.0011\ \text{day}^{-1}$ in the lymph, and up to $c = 0.020\ \text{day}^{-1}$ in the lung). Thus, the model-predicted median profiles showed a more stable dynamics of the lymph tumor and, to a lesser extent, in the lung and locoregionally (Supplementary Figure S5, available at https://doi.org/10.1016/j.esmoop.2021.100346).

When a tumor escaped treatment, the model assumed it followed its pre-treatment growth rate. This natural growth rate was higher in the liver (population median $g = 0.0052\ \text{day}^{-1}$), about five times larger than in the lymph, the lung or locoregionally ($g = 0.0009\ \text{day}^{-1}$, $0.0014\ \text{day}^{-1}$ or $0.0011\ \text{day}^{-1}$, respectively). Hence, the liver tumor median profiles showed an exponential growth in the tumor size, with a substantial impact of atezolizumab treatment due to the longer duration of effect (Supplementary Figure S5, available at https://doi.org/10.1016/j.esmoop.2021.100346). Indeed, treatment effect was more durable under atezolizumab in the lung and in the liver, with a $c$ parameter (resistance appearance rate) decreased by 57% ($P$ value $= 0.043$) and by 90% ($P$ value $= 0.001$) compared to chemotherapy, respectively (Table 2).

Consequently, the predicted tumor-size progression-free survival dropped very rapidly in patients having target

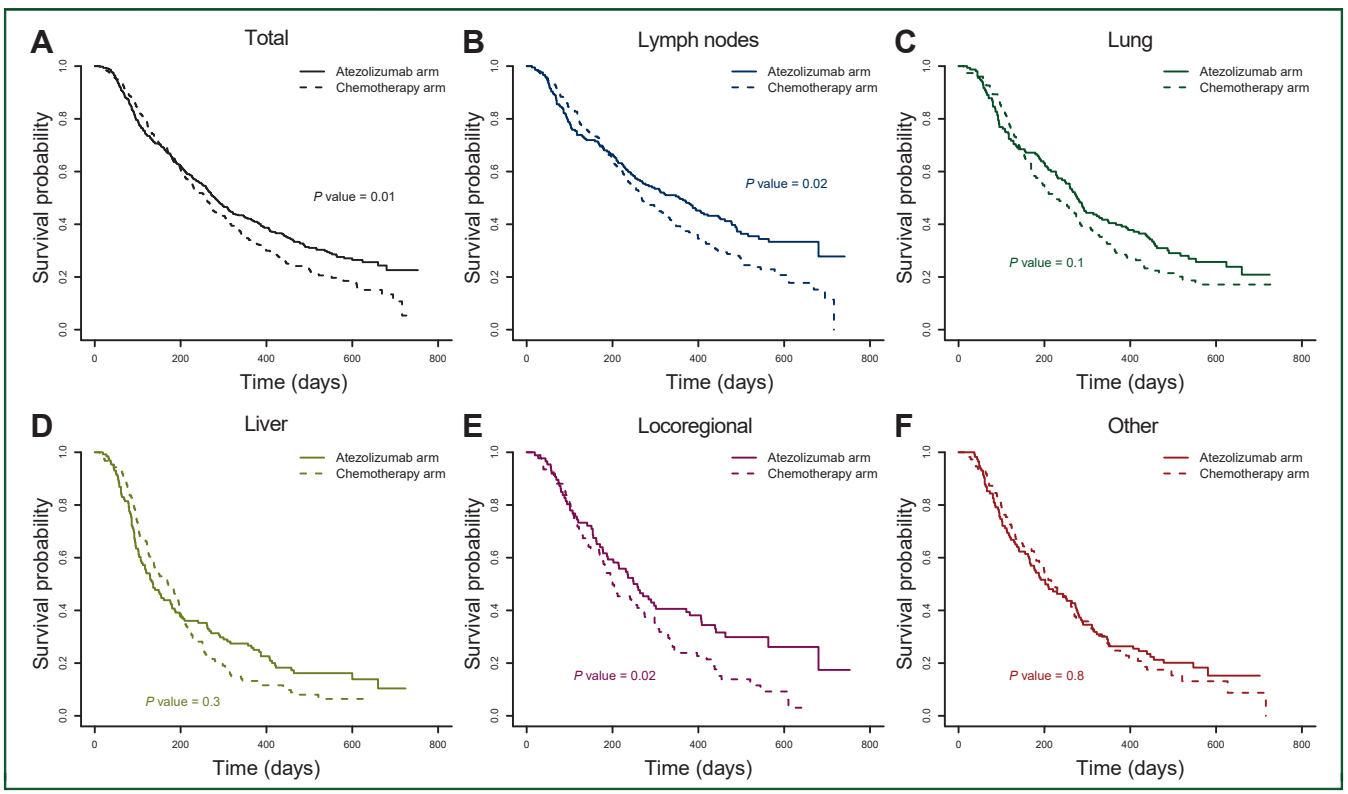


**Figure 1. Kaplan–Meier estimates of survival probability. (A) In the analysis population. (B), (C), (D), (E) and (F) In patients having at least one target lesion in the lymph node, lung, liver, locoregionally and in the other location. Survival is shown as solid lines in the atezolizumab arm and as dashed lines in the chemotherapy control arm.**

lesions in the liver (71 days to reach 50%), compared to the lung or locoregionally (between 120 and 180 days depending on treatment to reach 50%) (Figure 2). In contrast, lymph nodes tumor showed a longer tumor-size progression-free survival (221 days to reach 50%).

Overall, survival was initially larger in patients treated with chemotherapy who experienced a benefit early during the treatment period. Later in the study, as non-responding and relapsing patients dropped out, we observed a more beneficial and durable treatment effect in patients treated with atezolizumab (Figure 2). As an illustration, in the lung, at 100 days after treatment initiation, the tumor-size progression-free survival was about 79% in the chemotherapy arm versus 71% in the atezolizumab arm. However, at 400 days, it dropped to 21% in the chemotherapy arm versus 27% in the atezolizumab arm.

### *Overall survival model*

After adjusting on baseline covariates and atezolizumab effects, we calculated the association, noted $\beta_m$, between the tumor size in organ *m* and the instantaneous risk of death (hazard function). The tumor size in lymph nodes, lung, liver and locoregionally were all significantly associated with the hazard function (all *P* values $<0.05$, Walt test), meaning that an increase in the tumor size in any of these locations was associated with an increased risk of death.

However, the impact of the tumor dynamics depended on the tumor location, with values of $\beta_m$ varying from 0.0049 $mm^{-1}$ in the lung to as much as 0.011 $mm^{-1}$ in the liver (Table 2). Another way at looking at these results is to calculate the relative increase in the instantaneous risk of death caused by an increase of 10 mm in tumor size, given by $exp(10 \times \beta_m)$. All things being equal otherwise, the relative increase in the instantaneous risk of death caused by an increase of 10 mm of the tumor was equal to 12% (95% CI: 10% to 14%) and 10% (95% CI: 7.6% to 12.4%) for a lesion located in the liver and locoregionally, respectively. However, it was only 7% (95% CI: 4.6% to 9.4%) and 5% (95% CI: 3.3% to 6.7%) when the lesion is located in the lymph and the lung, respectively, showing that the impact of tumor dynamics greatly depends on the tumor location.

The importance of organ location to predict survival was also confirmed by comparing the adequation to the data of our model with the total SLD model, which assumes a similar level of association, $\beta$, between tumor dynamics and survival, irrespective of their location ($\beta = \beta_{lymph} = \beta_{lung} = \beta_{liver} = \beta_{locoregional}$). Our model had significantly improved the fit of survival data, with a decrease of 49.96 in BIC assuming organ-weighted associations compared to a single association (corresponding here to a *P* value $<10^{-14}$ in a likelihood ratio test, see Supplementary Table S1 in Supplementary Material, available at https://doi.org/10.1016/j.esmoop.2021.100346). The model showed good fit to the

**Table 2. Estimates (relative standard errors) of organ-specific SLD joint model population parameters**

| Models | Total SLD | Organ-specific SLD | | | | |
|---|---|---|---|---|---|---|
| | | Lymph nodes | Lung | Liver | Locoregional | Other |
| Longitudinal submodel | | | | | | |
| Fixed-effects parameters | | | | | | |
| $\mu_{BSLD}$ (mm) | 55.03 (2) | 31.9 (3) | 33.2 (4) | 40.4 (4) | 46.7 (4) | 41.8 (4) |
| Albumin concentration (g/l) | −0.016 (27)* | — | −0.024 (30)* | — | −0.0016 (49)** | — |
| C-reactive protein concentration (mg/l) | 0.0038 (14)* | 0.0015 (40)* | — | 0.0029 (27)* | 0.0023 (41)* | — |
| Lactate dehydrogenase value (U/l) | 0.00044 (24)* | — | — | 0.00035 (35)* | — | — |
| $\mu_g$ ($day^{-1}$) | 0.0023 (6) | 0.0009 (28) | 0.0014 (24) | 0.0052 (12) | 0.0011 (26) | 0.0011 (46) |
| Hemoglobin concentration (g/l) | −0.023 (14)* | −0.016 (50)** | −0.020 (39)** | — | — | — |
| $\mu_\varepsilon$ ($day^{-1}$) | 0.0067 (10) | 0.0050 (15) | 0.0039 (37) | 0.0020 (46) | 0.0017 (112) | 0.00047 (86) |
| Immunotherapy effect | −0.88 (15)* | — | −0.72 (49)** | — | — | — |
| $\mu_c$ ($day^{-1}$) | 0.023 (15) | 0.0011 (17) | 0.020 (34) | 0.0068 (43) | 0.037 (148) | 0.0072 (108) |
| Immunotherapy effect | −1.44 (14)* | — | −0.85 (50)** | −2.27 (31)* | — | — |
| Inter-patient variability | | | | | | |
| $\omega_{BSLD}$ | 0.64 (3) | 0.54 (4) | 0.65 (4) | 0.58 (5) | 0.51 (7) | 0.61 (5) |
| $\omega_g$ | 1.10 (5) | 1.21 (15) | 0.96 (14) | 0.56 (16) | 0.64 (38) | 1.01 (36) |
| $\omega_\varepsilon$ | 0.93 (5) | 1.06 (10) | 1.57 (14) | 1.74 (19) | 2.4 (31) | 2.71 (19) |
| $\omega_c$ | 1.23 (8) | 0.80 (20) | 0.85 (22) | 1.24 (27) | 3.53 (24) | 2.49 (24) |
| Survival submodel | | | | | | |
| Baseline hazard function parameters | | | | | | |
| K | 1.45 (7) | | | 1.48 (4) | | |
| Immunotherapy effect | −0.28 (26)* | | | −0.25 (22)* | | |
| $\lambda$ ($day^{-1}$) | 627 (7) | | | 573 (6) | | |
| Baseline survival covariates | | | | | | |
| Immunotherapy effect | −0.50 (18)* | | | −0.41 (21)* | | |
| ECOG score = 1 | 0.41 (16)* | | | 0.41 (20)* | | |
| Alkaline phosphatase concentration (U/L) | 0.0016 (20)* | | | 0.0013 (22)* | | |
| Neutrophil-to-lymphocyte ratio | 0.042 (16)* | | | 0.036 (22)* | | |
| Hemoglobin concentration ($g \cdot L^{-1}$) | −0.015 (18)* | | | −0.019 (16)* | | |
| Link parameter for *SLD* dynamics | | | | | | |
| $\beta$ ($mm^{-1}$) | 0.0076 (8)* | 0.0069 (21)* | 0.0049 (14)* | 0.011 (10)* | 0.0099 (14)* | — |

Wald test: *$P$ value $< 0.005$; **$P$ value $< 0.05$.
BSLD, baseline sum of longest diameter; ECOG, Eastern Cooperative Oncology Group; SLD, sum of the longest diameters.

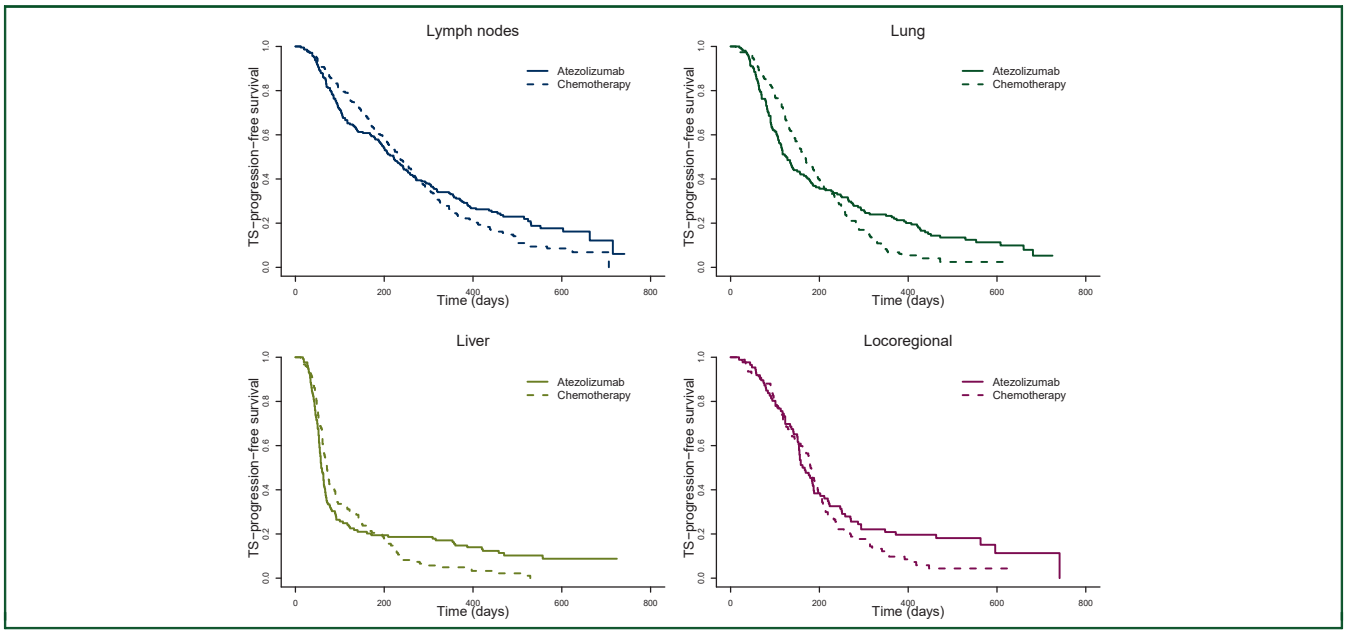


**Figure 2.** **Kaplan−Meier curves of model-predicted tumor-size (TS) progression-free survival in each location versus total in the atezolizumab arm (solid lines) and in the chemotherapy arm (dashed lines); the event is defined as a 20% increase above the nadir measurement or death, whichever comes first.**

data with satisfying goodness-of-fit assessment graphs for both longitudinal and survival data (Supplementary Figures S7-S10, available at https://doi.org/10.1016/j.esmoop.2021.100346).

### *Organ-specific tumor size for survival outcome prediction*

Joint model parameters were re-estimated successively using only data available at 3 months, 6 months and 9 months after the last patient inclusion, and survival data were simulated from those parameters estimates (see methods). Then, the simulated survival data were analyzed using a Cox regression model to evaluate the benefit of tumor size follow-up in the prediction of the survival trial outcome at 13 months after last patient inclusion. In the observed truncated data, the proportion of deaths was similar in both arms in the 3-month cut-off data with about 49% of death and the 95% confidence interval of the HR containing 1 [HR = 0.96 95% CI (0.80-1.16)] using a Cox regression model. The survival curves were slightly different in the 6-month cut-off data with about 62% of death in the chemotherapy arm and 56% in the atezolizumab arm, but no significant difference in survival was found between treatments yet at that time [HR = 0.89, 95% CI (0.75-1.05)]. At 9 months cut-off, the Cox HR was close to exclude 1 from its CI [HR = 0.86, 95% CI (0.73-1.01)].

Interestingly, using survival data simulated from the organ-specific SLD model, we predicted the significance of treatment effect at 6 months cut-off. On the contrary, no significant treatment effect was observed in the survival data simulated from the total SLD model. Using 9 months cut-off, both simulated data predicted a significant treatment effect using the Cox regression model; while applied to the 9 months truncated data, it showed no significant difference in survival between treatments (Figure 3).

## DISCUSSION

In oncology clinical trials, patient follow-up for treatment efficacy is commonly based on RECIST which consists of following over time the SLD of the different target lesions. Recently, several studies have suggested the existence of dissociated responses in target lesions, suggesting that relying on SLD could mask discrepancies in the response to treatment.[13,25] This might be particularly visible during immunotherapy, where the intra-patient variability could be exacerbated.[8,9] In parallel, the presence of metastasis in some organs, such as liver, has long been established as a factor of negative prognosis.[26,27] Here, relying on an exceptionally rich dataset of 900 patients with advanced or metastatic bladder cancer, we aimed to analyze in detail the heterogeneity in lesion dynamics across organs, as well as their marginal effects on survival.

The sTGI model proposed by Claret et al.[21] was preferred over alternative tumor growth models[28] for the sake of interpretability and estimate stability. We showed that the dynamics were very different across organs, irrespective of treatment received, and hold for all parameters characterizing the tumor dynamics, including the natural tumor growth rate ($g$ parameter). In general, lesions in the lymph nodes and the lung were durably affected by treatment, while the majority of lesions in the liver poorly responded to treatment. Consistent with observations made on the SLD level,[24] a higher proportion of patients showed an initial response to chemotherapy than to immunotherapy at the organ level (Figure 2). However, over time, the proportion of patients that maintained a response was larger in individuals treated with atezolizumab. This feature was captured in our model by a greater durability of treatment efficacy ($c$ parameter) in atezolizumab-treated patients, especially in the lung and the liver ($P$ values = 0.043 and

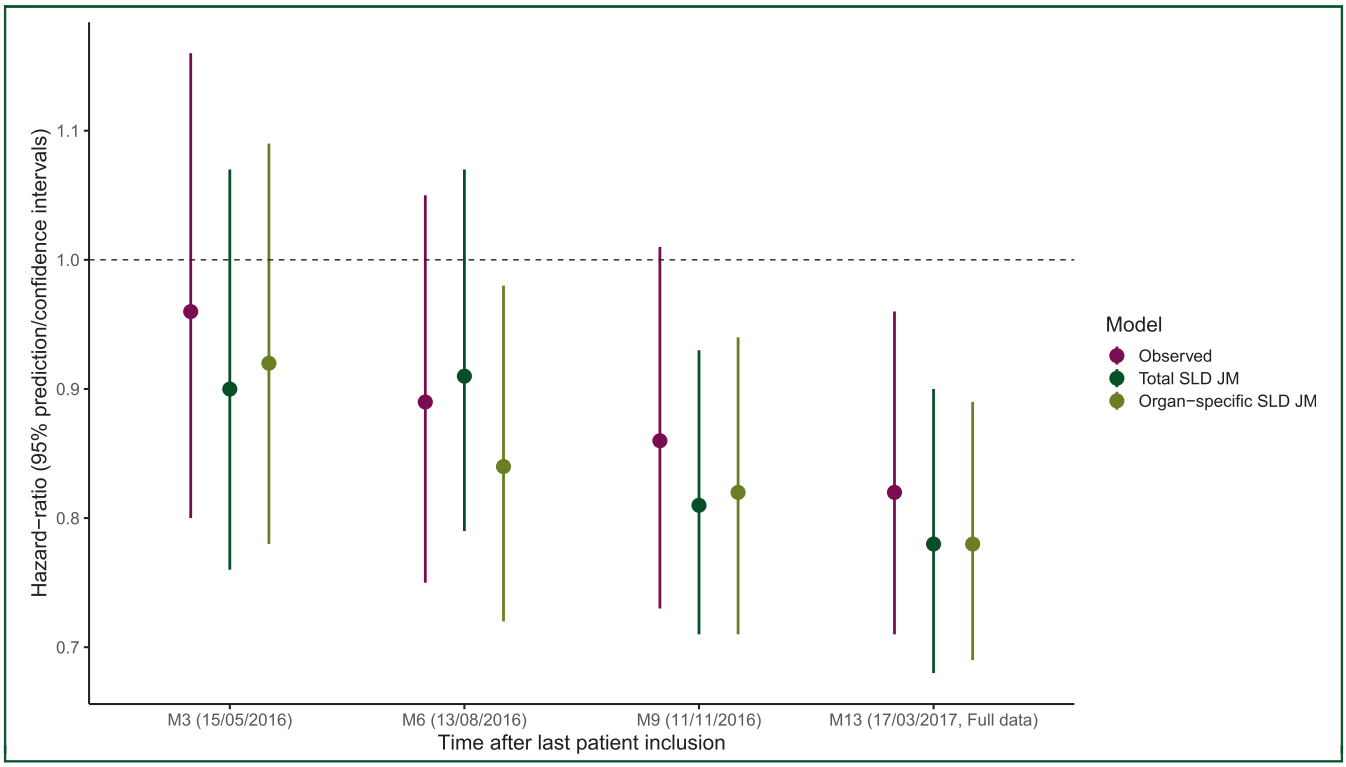


**Figure 3.** **Hazard ratio and its 95% confidence interval using Cox model on the full or truncated data compared to replicated hazard ratios and its 95% predictive interval based on total sum of the longest diameters (SLD) and organ-specific SLD joint model (JM) estimates.**

0.001, respectively). Of note, we did not test any interaction between baseline covariates and atezolizumab effects in our model, which might be investigated in future work. As immunotherapy currently revolutionizes the treatment of cancer patients, this new approach might help better understand the phenomenon of hyperprogression, whereby some patients experience an exacerbated tumor growth under immunotherapy. Indeed, recent study showed a significant association between liver metastases and hyperprogression,[29] suggesting a potential impact of the lesion location on the occurrence of such a phenomenon. This investigation will require both pre-treatment and post-treatment tumor size assessments,[8,30] which were not available in this study.

In addition to lesion dynamics being strongly organ dependent, our analysis revealed that the marginal impact of these lesions on survival was different. The association between lesion size in organ $m$ and the instantaneous rate of death, as measured by the parameter $\beta_m$, could vary in a onefold-to-twofold range, with the impact of lesions in the liver being twice as much detrimental than lesions located in the lung (Table 2). Of note, these results were not sensitive to the choice of structural model (see Supplementary Table S2 in Supplementary Material, available at https://doi.org/10.1016/j.esmoop.2021.100346). This importance of lesion location was confirmed by the comparison of data fitting between this model and a model assuming a similar impact of all lesions on survival (i.e. all $\beta_m$ being equal), which led to a highly significant deterioration of the likelihood function ($P$ value $<10^{-14}$).

Finally, we evaluated the model in a prospective manner to anticipate study outcome. Following an approach developed by Claret et al.,[24] we showed that the outcome could be predicted 6 months after last patient, i.e. as early as 6 months before the final cut-off date used for data analysis.[20] This is better than what could be obtained by a similar model relying on SLD, where treatment outcome could only be predicted 9 months after inclusion of the last patient. Although this internal validation should not be over interpreted, it suggests that the analysis of all available information, including tumor location, provides more statistical power to detect a benefit of treatment effect on tumor dynamics, which will eventually translate into a sensible benefit on survival.

Of note, our model did not show any benefit to identify most at-risk patients during follow-up over a model relying on SLD,[19] which suggests that individual lesions may be more informative at the population level than at the individual level. This may illustrate the limitations of relying only on target lesion dynamics, while important sources of information were not accounted for, such as the appearance of new lesions, the dynamics of non-target lesions[31] or the drug pharmacokinetics.[32] Incorporating these information will be particularly challenging, and will require to develop more complex models of drug response that address more efficiently the correlation between the lesion dynamics. This can be done, for instance, by adding an additional level of random effects to better delineate the between-patient variability from the intra-patient variability, as was recently proposed in the context of linear models.[33]

## FUNDING

This work received financial support from the French National Agency for Research and Technology (ANRT), France, Genentech Clinical Pharmacology, USA and Roche Institute, France (no grant number).

## DISCLOSURE

MK, FM, AL, BW, JJ, XS and RB are Roche/Genentech employees. JG and SD have been consultant for Roche on other projects. CLT has participated in advisory boards from Roche, MSD, BMS, Merck Serono, AstraZeneca, Rakuten, Seattle Genetics, Nanobiotix, GSK and Celgene.

## REFERENCES

1. Survival Rates for Bladder Cancer. Available at https://www.cancer.org/cancer/bladder-cancer/detection-diagnosis-staging/survivalrates.html. Accessed September 8, 2020.
2. Bellmunt J, de Wit R, Vaughn DJ, et al. Pembrolizumab as second-line therapy for advanced urothelial carcinoma. *N Engl J Med*. 2017;376:1015-1026.
3. Reck M, Rodríguez-Abreu D, Robinson AG, et al. Pembrolizumab versus chemotherapy for PD-L1—positive non—small-cell lung cancer. *N Engl J Med*. 2016;375:1823-1833.
4. Mok TSK, Wu YL, Kudaba I, et al. Pembrolizumab versus chemotherapy for previously untreated, PD-L1-expressing, locally advanced or metastatic non-small-cell lung cancer (KEYNOTE-042): a randomised, open-label, controlled, phase 3 trial. *Lancet*. 2019;393:1819-1830.
5. Powles T, Park SH, Voog E, et al. Avelumab maintenance therapy for advanced or metastatic urothelial carcinoma. *N Engl J Med*. 2020;383:1218-1230.
6. Powles T, Eder JP, Fine GD, et al. MPDL3280A (anti-PD-L1) treatment leads to clinical activity in metastatic bladder cancer. *Nature*. 2014;515:558-562.
7. Frelaut M, du Rusquec P, de Moura A, Le Tourneau C, Borcoman E. Pseudoprogression and hyperprogression as new forms of response to immunotherapy. *BioDrugs*. 2020;34:463-476.
8. Borcoman E, Kanjanapan Y, Champiat S, et al. Novel patterns of response under immunotherapy. *Ann Oncol*. 2019;30:385-396.
9. Vera-Yunca D, Girard P, Parra-Guillen ZP, Munafo A, Trocóniz IF, Terranova N. Machine learning analysis of individual tumor lesions in four metastatic colorectal cancer clinical studies: linking tumor heterogeneity to overall survival. *AAPS J*. 2020;22:58.
10. Terranova N, Girard P, Ioannou K, Klinkhardt U, Munafo A. Assessing similarity among individual tumor size lesion dynamics: the CICIL methodology. *CPT Pharmacomet Syst Pharmacol*. 2018;7:228-236.
11. Halabi S, Kelly WK, Ma H, et al. Meta-analysis evaluating the impact of site of metastasis on overall survival in men with castration-resistant prostate cancer. *J Clin Oncol*. 2016;34:1652-1659.
12. Eisenhauer EA, Therasse P, Bogaerts J, et al. New response evaluation criteria in solid tumours: revised RECIST guideline (version 1.1). *Eur J Cancer*. 2009;45:228-247.
13. Mercier F, Kerioui M, Desmée S, Guedj J, Krieter O, Bruno R. Longitudinal analysis of organ-specific tumor lesion sizes in metastatic colorectal cancer patients receiving first line standard chemotherapy in combination with anti-angiogenic treatment. *J. Pharmacokinet. Pharmacodyn*. 2020;47:613-625.
14. Bruno R, Bottino D, de Alwis DP, et al. Progress and opportunities to advance clinical cancer therapeutics using tumor dynamic models. *Clin Cancer Res*. 2020;26:1787-1795.
15. Wulfsohn MS, Tsiatis AA. A joint model for survival and longitudinal data measured with error. *Biometrics*. 1997;53:330-339.
16. Rizopoulos D. *Joint models for longitudinal and time-to-event data: with applications in R*. Boca Raton: CRC Press; 2012.
17. Desmée S, Mentré F, Veyrat-Follet C, Guedj J. Nonlinear mixed-effect models for prostate-specific antigen kinetics and link with survival in the context of metastatic prostate cancer: a comparison by simulation of two-stage and joint approaches. *AAPS J*. 2015;17:691-699.
18. Rosenberg JE, Hoffman-Censits J, Powles T, et al. Atezolizumab in patients with locally advanced and metastatic urothelial carcinoma who have progressed following treatment with platinum-based chemotherapy: a single-arm, multicentre, phase 2 trial. *Lancet*. 2016;387:1909-1920.
19. Tardivon C, Desmée S, Kerioui M, et al. Association between tumor size kinetics and survival in patients with urothelial carcinoma treated with atezolizumab: implication for patient follow-up. *Clin Pharmacol Ther*. 2019;106:810-820.
20. Powles T, Durán I, van der Heijden MS, et al. Atezolizumab versus chemotherapy in patients with platinum-treated locally advanced or metastatic urothelial carcinoma (IMvigor211): a multicentre, open-label, phase 3 randomised controlled trial. *Lancet*. 2018;391:748-757.
21. Claret L, Gupta M, Han K, et al. Evaluation of tumor-size response metrics to predict overall survival in Western and Chinese patients with first-line metastatic colorectal cancer. *J Clin Oncol*. 2013;31:2110-2114.
22. Kuhn E, Lavielle M. Maximum likelihood estimation in nonlinear mixed effects models. *Comput Stat Data Anal*. 2005;49:1020-1038.
23. Nguyen THT, Mouksassi MS, Holford N, et al. Model evaluation of continuous data pharmacometric models: metrics and graphics. *CPT Pharmacomet Syst Pharmacol*. 2017;6:87-109.
24. Claret L, Jin JY, Ferté C, et al. A Model of overall survival predicts treatment outcomes with atezolizumab versus chemotherapy in non—small cell lung cancer based on early tumor kinetics. *Clin Cancer Res*. 2018;24:3292-3298.
25. Schindler E, Amantea MA, Karlsson MO, Friberg LE. PK-PD modeling of individual lesion FDG-PET response to predict overall survival in patients with sunitinib-treated gastrointestinal stromal tumor. *CPT Pharmacomet Syst Pharmacol*. 2016;5:173-181.
26. Hegde PS, Chen DS. Top 10 challenges in cancer immunotherapy. *Immunity*. 2020;52:17-35.
27. Tumeh PC, Hellmann MD, Hamid O, et al. Liver metastasis and treatment outcome with anti-PD-1 monoclonal antibody in patients with melanoma and NSCLC. *Cancer Immunol Res*. 2017;5:417-424.
28. Stein WD, Yang J, Bates SE, Fojo T. Bevacizumab reduces the growth rate constants of renal carcinomas: a novel algorithm suggests early discontinuation of evacizumab resulted in a lack of survival advantage. *Oncologist*. 2008;13:1055-1062.
29. Sasaki A, Nakamura Y, Mishima S, et al. Predictive factors for hyperprogressive disease during nivolumab as anti-PD1 treatment in patients with advanced gastric cancer. *Gastric Cancer*. 2019;22:793-802.
30. Ferrara R, Mezquita L, Texier M, et al. Hyperprogressive disease in patients with advanced non—small cell lung cancer treated with PD-1/PD-L1 inhibitors or with single-agent chemotherapy. *JAMA Oncol*. 2018;4:1543-1552.
31. Król A, Ferrer L, Pignon JP, et al. Joint model for left-censored longitudinal data, recurrent events and terminal event: predictive abilities of tumor burden for cancer evolution with application to the FFCD 2000-05 trial. *Biometrics*. 2016;72:907-916.
32. Netterberg I, Li CC, Molinero L, et al. A PK/PD analysis of circulating biomarkers and their relationship to tumor response in atezolizumab-treated non-small cell lung cancer patients. *Clin Pharmacol Ther*. 2019;105:486-495.
33. Brilleman SL, Crowther MJ, Moreno-Betancur M, et al. Joint longitudinal and time-to-event models for multilevel hierarchical data. *Stat Methods Med Res*. 2019;28:3502-3515.